Journal of Clinical and Translational Hepatology **2025** vol. 13(12) | 1046–1059
DOI: 10.14218/JCTH.2025.00343

Original Article

PDK4 Regulates Inflammatory Injury in Acute-on-chronic Liver Failure by Phosphorylating STAT1-mediated M1 Polarization of Macrophages

Shilong Dong[1,2,3#], Luyuan Ma[1,2,3#], Chuan Shen[1,2,3], Ruolan Gu[1,2,3], Xinyang Li[1,2,3], Ying Xiao[1,2,3] and Caiyan Zhao[1,2,3*]

[1]Department of Infectious Diseases, Hebei Medical University Third Hospital, Shijiazhuang, Hebei, China; [2]Clinical Research Center for Infectious Disease of Hebei Province, Shijiazhuang, Hebei, China; [3]Hebei Key Laboratory for Diagnosis, Treatment, Emergency Prevention and Control of Critical Infectious Diseases, Shijiazhuang, Hebei, China

Received: July 13, 2025 | **Revised:** October 01, 2025 | **Accepted:** November 12, 2025 | **Published online:** November 26, 2025

Abstract

Background and Aims: Acute-on-chronic liver failure (ACLF) is a life-threatening syndrome characterized by systemic inflammation and immune dysregulation, in which macrophages play a key role in organ injury. This study aimed to investigate the role and mechanism of pyruvate dehydrogenase kinase 4 (PDK4) in ACLF to identify therapeutic targets that modulate macrophage function and mitigate ACLF progression. ***Methods:*** Single-cell RNA sequencing data from healthy and ACLF liver tissues were analyzed from the Sequence Read Archive database. Transcriptomic data of peripheral blood mononuclear cells from ACLF patients (GSE168048) were also examined. *In vitro* experiments assessed PDK4 expression and macrophage polarization, and conditioned-medium studies evaluated effects on LO2 hepatocytes. *In vivo* validation was performed in ACLF mouse models treated with a PDK4 inhibitor. ***Results:*** Single-cell analysis revealed a predominance of M1-polarized hepatic macrophages in ACLF with marked upregulation of PDK4. Peripheral blood mononuclear cell transcriptomics showed that higher PDK4 expression correlated with 28-day mortality. *In vitro*, PDK4 expression increased in M1 macrophages; PDK4 inhibition attenuated M1 polarization and reduced cytotoxic effects on LO2 cells. *In vivo*, pharmacologic inhibition of PDK4 suppressed M1 polarization in macrophages, alleviated liver inflammation, and reduced tissue injury. Mechanistically, PDK4 promoted M1 polarization via activation of signal transducer and activator of transcription 1 signaling. ***Conclusions:*** PDK4 is a key pro-inflammatory regulator in ACLF by promoting M1 macrophage polarization. Targeting PDK4 may be a promising strategy to attenuate inflammation and improve clinical outcomes in ACLF.

Keywords: Acute-on-chronic liver failure; Pyruvate dehydrogenase kinase 4; Inflammation; Macrophage; M1 polarization; Signal transducer and activator of transcription 1.

[#]Contributed equally to this work.

[*]**Correspondence to:** Caiyan Zhao, Department of Infectious Diseases, Hebei Medical University Third Hospital, 168 Xiangjiang Road, Shijiazhuang, Hebei 050000, China. ORCID: https://orcid.org/0000-0001-5997-4641. Tel: +86-311-66776873, E-mail: zhaocy@hebmu.edu.cn

Citation of this article: Dong S, Ma L, Shen C, Gu R, Li X, Xiao Y, *et al*. PDK4 Regulates Inflammatory Injury in Acute-on-chronic Liver Failure by Phosphorylating STAT1-mediated M1 Polarization of Macrophages. J Clin Transl Hepatol 2025;13(12):1046–1059. doi: 10.14218/JCTH.2025.00343.

Introduction

Acute-on-chronic liver failure (ACLF) is a severe clinical syndrome characterized by rapid deterioration of liver function in patients with pre-existing chronic liver disease following acute insults.[1] Although definitions and diagnostic criteria for ACLF vary across regions, consensus highlights its high mortality.[2,3] Globally, approximately 35% of hospitalized patients with decompensated cirrhosis develop ACLF, with an approximately 60% 90-day survival rate.[4] Current treatment strategies primarily focus on organ support and management of complications. Although artificial liver support systems and liver transplantation have improved prognosis for some patients, high plasma consumption, elevated costs, increased risks of infection and bleeding, donor organ shortages, and postoperative complications remain substantial barriers.[5] There is an urgent need to identify effective prognostic biomarkers and explore novel therapeutic strategies to improve outcomes in patients with ACLF.

Emerging evidence indicates that systemic inflammation and immune dysregulation are key drivers of ACLF development and progression. Macrophages have been shown to drive inflammatory progression in various models of liver injury, including ACLF.[6,7] Macrophages exhibit remarkable heterogeneity and plasticity, and they can polarize into pro-inflammatory M1 or anti-inflammatory/tissue-repairing M2 phenotypes in response to distinct microenvironmental cues.[8] Numerous studies have demonstrated that modulating macrophage polarization to attenuate its pro-inflammatory functions represents a promising therapeutic strategy for alleviating hepatic inflammation.[9,10] Signal transducer and activator of transcription 1 (STAT1) is a key transcription factor regulating M1 polarization and is primarily activated through phosphorylation in response to interferon-gamma (IFN-γ) and other inflammatory stimuli. Once activated, STAT1 translocates to the nu-

cleus and promotes transcription of pro-inflammatory genes such as iNOS, IL-6, and TNF-α, thereby driving macrophages toward the M1 phenotype.[11] During the early stages of ACLF, both M1 and M2 macrophage subsets are activated; however, heightened pro-inflammatory activity of M1 macrophages leads to excessive production of inflammatory cytokines, contributing to hepatic injury and multiple organ failure.[12]

PDK4, a member of the pyruvate dehydrogenase kinase family, is widely expressed in various tissues, including the heart, liver, and skeletal muscle. It plays a pivotal role in cellular metabolism by phosphorylating specific serine residues on the pyruvate dehydrogenase E1 alpha subunit (PDHE1α), thereby inhibiting its activity. This prevents conversion of pyruvate to acetyl-CoA, limits entry of glucose into mitochondrial oxidative metabolism, and promotes glycolysis.[13] Previous studies have primarily examined the role of PDK4 in metabolic diseases such as cancer, diabetes, and atherosclerosis.[14,15] More recently, evidence indicates that PDK4 can also modulate inflammatory responses by regulating immune cell metabolism.[16] However, the role of PDK4 in the pathogenesis of ACLF remains largely unknown.

This study investigates the function and underlying mechanisms of PDK4 in ACLF. Through multi-omics analysis, we found that PDK4 was significantly upregulated in hepatic macrophages and peripheral blood mononuclear cells (PBMCs) from patients with ACLF, and its expression levels were closely associated with disease severity and short-term mortality. Further experiments demonstrated that PDK4 promoted macrophage polarization toward the M1 phenotype, whereas PDK4 inhibition effectively alleviated liver inflammation and tissue injury in an ACLF mouse model. Mechanistically, PDK4 facilitated M1 polarization by enhancing STAT1 phosphorylation. Collectively, these findings reveal a critical role for PDK4 in regulating macrophage polarization and exacerbating liver injury in ACLF, and identify PDK4 as a potential therapeutic target for ACLF treatment.

Methods

Public transcriptomic data acquisition and analysis

The Gene Expression Omnibus (GEO; https://www.ncbi.nlm.nih.gov/geo/) datasets GSE168048 and GSE142255, and the Sequence Read Archive (SRA) BioProject PRJNA913603 (https://www.ncbi.nlm.nih.gov/bioproject/PRJNA913603) were used as data sources in this study.

The GSE168048 dataset contains transcriptomic data from PBMCs of 16 patients with ACLF, including eight non-survivors and eight survivors based on 28-day outcomes. The GSE142255 dataset comprises whole-blood transcriptomic data from 17 ACLF patients and seven healthy controls (HCs). The SRA BioProject PRJNA913603 provides single-cell RNA sequencing (scRNA-seq) data derived from liver tissues of five ACLF patients and three HCs.

Bulk RNA-seq data (GSE168048, GSE142255) were analyzed using GEO2R to identify differentially expressed genes (DEGs) between ACLF patients and HCs, or between 28-day non-survivors and survivors ($|\log_2 FC| > 1$, $P < 0.05$). scRNA-seq data from SRA (PRJNA913603) were processed using Celescope v2.0.7 (Singleron) for demultiplexing, UMI counting, and alignment to the GRCh38 reference genome. Quality control and integration were performed in Seurat (v5.0.1),[17] retaining cells with ≥200 detected genes, UMI counts below the 95th percentile, and mitochondrial content ≤ 15%. After normalization and variable gene selection, reciprocal PCA and FindIntegrationAnchors were used for data integration. PCA and clustering (resolution = 0.8) were conducted using RunPCA and FindClusters, respectively. Cell types were annotated using canonical markers. Macrophage-specific DEGs were identified with FindMarkers (adjusted $P < 0.05$, $|\log_2 FC| > 0.25$). Gene Ontology enrichment analysis was conducted using WebGestalt,[18] and significant pathways (FDR < 0.05) were visualized via bar plots of normalized enrichment scores.

Patient samples

PBMCs were collected from 22 patients with ACLF at the time of their initial hospital admission, prior to any medical intervention, and from six HCs between June 2023 and December 2024 at the Third Hospital of Hebei Medical University. In addition, liver tissue samples were collected from three patients with ACLF (resected during liver transplantation) and three control donors (normal liver tissues obtained during liver transplantation procedures). All ACLF patients received standardized medical management, including but not limited to etiological therapy, hepatoprotective and transaminase-lowering agents, nutritional support, and management of associated complications such as ascites, hepatic encephalopathy, and coagulopathy. The enrollment criteria for ACLF patients were defined according to the Guidelines for the Diagnosis and Treatment of Liver Failure (2018 Edition, China), which included the following key components: (I) acute deterioration occurring on the basis of pre-existing chronic liver disease; (II) serum total bilirubin ≥ 10 times the upper limit of normal or a daily increase > 17.1 μmol/L; (III) prothrombin activity ≤ 40% or international normalized ratio ≥ 1.5. The exclusion criteria included: (I) age < 18 years or >80 years; (II) pregnancy; (III) concomitant hepatocellular carcinoma or other malignancies; (IV) severe extrahepatic diseases; (V) incomplete clinical data. This study protocol was approved by the Ethics Committee of the Third Hospital of Hebei Medical University (Ethical Approval Number: K2024-052-1). All research procedures were conducted in accordance with the Declaration of Helsinki. Informed consent was obtained from all participants.

Animal model and treatments

Male BALB/c mice (four weeks old) were purchased from Huafukang Bioscience (Beijing, China) and housed under SPF conditions at 22°C with 50% humidity and a 12-h light/dark cycle.

All animal experiments were approved by the Animal Ethics Committee of the Third Hospital of Hebei Medical University (Approval Number: Z2024-036-2).

An ACLF model was induced in mice by combined treatment with carbon tetrachloride (CCl_4), D-galactosamine (D-GalN), and lipopolysaccharide (LPS).[19] After one week of acclimatization, mice were randomly divided into three groups (n = 6 per group).Control group: received vehicle only. ACLF group: chronic liver injury was induced by intraperitoneal injection of 20% CCl_4 (5 mL/kg), twice weekly for 12 weeks. Acute exacerbation was triggered three days after the last dose by LPS (100 μg/kg, Sigma, USA) and D-GalN (0.5 g/kg, TargetMol). PDK4-IN group: same treatment as the ACLF group, plus oral administration of PDK4-IN-1 hydrochloride (PDK4-IN, 50 mg/kg, TargetMol, Shanghai, China) 8 h before LPS/D-GalN.[20] Six hours after acute stimulation, mice were anesthetized. Blood was collected via orbital puncture, and peritoneal macrophages were harvested by PBS lavage. Additionally, liver tissues were fixed in formaldehyde and embedded in paraffin for subsequent histopathological examination.

Cell culture and treatment

The human monocytic cell line THP-1, the murine macrophage

Table 1. Sequences of the primers used for quantitative real-time PCR

Gene	Forward primer (5′–3′)	Reverse primer (5′–3′)
Human		
PDK4	GGAGCATTTCTCGCGCTACA	ACAGGCAATTCTTGTCGCAAA
CD86	CTGCTCATCTATACACGGTTACC	GGAAACGTCGTACAGTTCTGTG
iNOS	TTCAGTATCACAACCTCAGCAAG	TGGACCTGCAAGTTAAAATCCC
IL-6	ACTCACCTCTTCAGAACGAATTG	CCATCTTTGGAAGGTTCAGGTTG
TNF-α	CCTCTCTCTAATCAGCCCTCTG	GAGGACCTGGGAGTAGATGAG
CD206	TCCTTGTGGGATTGTCCTGC	AAGCCGCTGTCTCTGTCTTC
β-actin	CATGTACGTTGCTATCCAGGC	CTCCTTAATGTCACGCACGAT
Mouse		
PDK4	AGGGAGGTCGAGCTGTTCTC	GGAGTGTTCACTAAGCGGTCA
CD86	TGTTTCCGTGGAGACGCAAG	TTGAGCCTTTGTAAATGGGCA
iNOS	ACATCGACCCGTCCACAGTAT	CAGAGGGGTAGGCTTGTCTC
IL-6	TAGTCCTTCCTACCCCAATTTCC	TTGGTCCTTAGCCACTCCTTC
TNF-α	AATGGCCTCCCTCTCATCAGTT	CCACTTGGTGGTTTGCTACGA
CD206	GTTCACCTGGAGTGATGGTTCTC	AGGACATGCCAGGGTCACCTTT
β-actin	GGCTGTATTCCCCTCCATCG	CCAGTTGGTAACAATGCCATGT

cell line RAW264.7, and the human hepatocyte cell line LO2 were purchased from Pricells Biotechnology (Wuhan, China). THP-1 and LO2 cells were cultured in RPMI-1640 medium (Gibco, NY, USA) supplemented with 10% fetal bovine serum, while RAW264.7 cells were maintained in high-glucose DMEM (Gibco, NY, USA) with 10% fetal bovine serum. All cells were incubated at 37°C in a humidified atmosphere with 5% CO_2. THP-1 cells were differentiated into THP-1 macrophages using phorbol 12-myristate 13-acetate (PMA, MCE, NJ, USA). THP-1 macrophages were polarized toward the M1 phenotype by stimulation with LPS (100 ng/mL, Sigma, MO, USA) and IFN-γ (20 ng/mL, Novoprotein, Suzhou, China) for 24 h, or into the M2 phenotype by treatment with IL-4 and IL-13 (both 20 ng/mL, MCE, NJ, USA) for 24 h.[21]

RAW264.7 cells were polarized into M1 macrophages by stimulation with 1 μg/mL LPS for 24 h,[22] or into M2 macrophages with 20 ng/mL IL-4 (MCE, NJ, USA) for 24 h.[23]

For PDK4 inhibition experiments, cells were pretreated with PDK4-IN at different concentrations (0.625, 2.5, and 5 μM) for 6 h, followed by LPS/IFN-γ stimulation to induce M1 polarization. For overexpression experiments, THP-1 macrophages were transfected with PDK4 overexpression plasmids (OE-PDK4) or empty vectors (OE-EV) using PolyJet™ transfection reagent (SignaGen Laboratories, MD, USA). After 24 h of transfection, cells were stimulated with LPS and IFN-γ to induce M1 polarization.

To investigate the effect of PDK4 on LO2 hepatocyte injury through the regulation of macrophage polarization, THP-1 macrophages were divided into three groups: Control, LPS/IFN-γ (L/I), and L/I + PDK4-IN. Following polarization induction, the culture medium was replaced with RPMI-1640 complete medium, and the cells were further incubated for 24 h. The supernatants were then collected, centrifuged to remove cellular debris, and mixed with complete RPMI-1640 medium at a 1:1 ratio for subsequent culture of LO2 cells.[24]

RNA extraction and quantitative real-time PCR (RT-qPCR)

Total RNA was extracted using TRIzol reagent (Invitrogen, CA, USA). Complementary DNA was synthesized using reverse transcription kits (Yeasen, Shanghai, China). RT-qPCR was performed using SYBR Green on an ABI 2000 system (Applied Biosystems, CA, USA). Each 20 μL reaction contained 10 μL 2× SYBR Green Master Mix, 0.5 μL forward primer, 0.5 μL reverse primer, and 9 μL diluted complementary DNA template. Relative gene expression was calculated using the $2^{-\Delta\Delta Ct}$ method, with target gene expression levels normalized to the housekeeping gene β-actin and presented as fold change relative to the control group.[25] Primer sequences are listed in Table 1.

Western blotting

Cells or tissues were lysed in RIPA buffer. Proteins were separated by SDS-PAGE and transferred to nitrocellulose membranes, followed by blocking with 5% non-fat milk. Membranes were incubated with primary antibodies against PDK4 (Proteintech, Wuhan, China), CD86 (Abmart, Wuhan, China), CD206 (Huabio, Hangzhou, China), iNOS (Huabio, Hangzhou, China), STAT1 (Huabio, Hangzhou, China), p-STAT1 (Abmart, Shanghai, China), p-PDHE1α (Huabio, Hangzhou, China), and β-tubulin (Abmart, Shanghai, China), followed by HRP-conjugated secondary antibodies (Abmart, Shanghai, China). Protein bands were visualized using enhanced chemiluminescence reagents.[26]

Flow cytometry

Flow cytometry was employed to assess the polarization status of THP-1 macrophages. In brief, cells were incubated with fluorophore-conjugated anti-CD86 antibody (M1 marker) in the dark for 20 m. After thorough washing, the cells were resuspended in buffer and analyzed using a CytoFLEX flow cytometer (Beckman Coulter, CA, USA) to determine the distribution of different macrophage phenotypes.[27]

Apoptosis of LO2 cells was also evaluated by flow cytometry. Briefly, LO2 cells were co-cultured with macrophage-conditioned medium for 24 h. After harvesting, Annexin V-FITC and propidium iodide were sequentially added, followed

by incubation in the dark for 20 m prior to flow cytometric analysis.[28]

Cell Counting Kit-8 (CCK-8) assay

The CCK-8 assay was conducted to detect changes in LO2 cell viability. LO2 cells were co-cultured with macrophage-conditioned medium for 24 h. Then, 10 μL CCK-8 reagent was added. After incubation for 4 h, the OD value was detected at 450 nm with a microplate reader, with blank culture medium as the control. Finally, cell viability was calculated, and results were expressed as percentages.[28]

Cellular immunofluorescence staining

Cells were seeded on coverslips, fixed with 4% paraformaldehyde for 15 m, permeabilized with 0.1% Triton X-100 for 10 m, and blocked with 5% BSA for 1 h. Cells were incubated overnight at 4°C with primary antibodies against CD68 and CD86 (Proteintech), followed by fluorophore-conjugated secondary antibodies. Nuclei were counterstained with DAPI. Images were captured using an Axioscope 5 fluorescence microscope (ZEISS, Germany), and fluorescence intensity was quantified using ImageJ software.[22]

Multiplex immunofluorescence immunohistochemistry

Liver tissues were fixed in 10% paraformaldehyde, embedded in paraffin, and sectioned. After deparaffinization and antigen retrieval, sections were blocked with 5% BSA and incubated with primary antibodies against PDK4 (Proteintech), CD68 (Abcam, Cambridge, UK), and CD86 (Abcam), followed by corresponding fluorophore-conjugated secondary antibodies. Nuclei were stained with DAPI. Images were captured with an Axioscope 5 fluorescence microscope (ZEISS).[29]

Enzyme-linked immunosorbent assay (ELISA)

Concentrations of IL-6 and TNF-α in culture supernatants and mouse serum were measured using human (Jonlnbio, Shanghai, China) and mouse (Thermo Fisher, MA, USA) ELISA kits, respectively.

Biochemical assays

Serum levels of alanine aminotransferase, aspartate aminotransferase, and total bilirubin were measured using an automatic biochemical analyzer (Rayto, Shenzhen, China) to evaluate liver function.

Histology and immunohistochemistry

Liver tissues were fixed in 10% formalin, embedded in paraffin, and sectioned for hematoxylin and eosin staining. For immunohistochemistry, sections were stained with antibodies against CD86 (Proteintech), followed by HRP-conjugated secondary antibodies and DAB development to assess the M1 polarization level.[30]

RNA-seq and gene set enrichment analysis (GSEA)

To investigate the mechanism by which PDK4 regulates macrophage polarization, two treatment conditions were established: macrophages stimulated with LPS/IFN-γ (control group) and macrophages pretreated with PDK4-IN (PDK4-IN-1 hydrochloride, TargetMol) for 6 h prior to LPS/IFN-γ stimulation (PDK4-IN group). Total RNA was extracted, and libraries were constructed for paired-end sequencing on the DNBSEQ platform. Raw sequencing reads were quality-controlled using SOAPnuke and aligned to the human genome (GRCh38) using HISAT2 (v2.2.1). Gene counting was performed using featureCounts. Differential expression analysis was conducted using DESeq2 (v1.40.2) with a significance threshold of Q value ≤ 0.05.[31] GSEA (gsea-3.0) was applied to rank genes based on $\log_2$ fold change ($\log_2$FC) and identify enriched pathways.[32] The gene set c2.cp.kegg.v6.2.symbols.gmt from the MSigDB (v6.2) database was used as a reference.[33]

Statistical analysis

All data are presented as mean ± standard deviation. Differences between two groups were assessed using unpaired Student's t-test, while comparisons among multiple groups were evaluated by one-way ANOVA followed by Tukey's post hoc test. Correlations were analyzed using Pearson's correlation coefficient. A P-value < 0.05 was considered statistically significant. Statistical analyses were performed using GraphPad Prism 10 (GraphPad, San Diego, CA, USA).

Results

scRNA-seq reveals M1-like polarization predisposition in early-stage ACLF liver macrophages

We systematically analyzed publicly available scRNA-seq data (PRJNA913603) from liver biopsies of five patients with ACLF and three HCs. UMAP visualization identified multiple non-parenchymal cell populations, including macrophages, monocytes, T cells, B cells, mast cells, neutrophils, fibroblasts, endothelial cells, epithelial cells, blood cells, and cycling cells. Notably, distinct clustering patterns were observed between ACLF and HC samples (Fig. 1A and B).

DEG analysis of hepatic macrophages revealed 569 upregulated and 710 downregulated genes in patients with ACLF compared with HCs (Fig. 1C). Gene Ontology enrichment analysis of the upregulated genes showed significant activation of immune-related pathways, including type I interferon signaling, IFN-γ response, and antigen processing and presentation (Fig. 1D). Taken together, these findings suggest that liver macrophages in early-stage ACLF may exhibit a predisposition toward pro-inflammatory, M1-like polarization.

Elevated PDK4 expression in PBMCs and hepatic tissues correlates with adverse clinical outcomes in ACLF patients

To identify genes associated with ACLF pathogenesis and prognosis, we analyzed multiple transcriptomic datasets. In the whole-blood dataset GSE142255, 164 genes were upregulated and 224 were downregulated in patients with ACLF compared with HCs (Fig. 2A). In the PBMC dataset GSE168048, 837 genes were upregulated and 631 were downregulated when comparing 28-day non-survivors with survivors (Fig. 2B). To further screen candidate genes in macrophages, we applied more stringent criteria (absolute $\log_2$ fold change > 1, P < 0.05) to scRNA-seq data, identifying 139 upregulated and 389 downregulated genes (Fig. 2C). Integrating the DEGs from GSE142255, GSE168048, and macrophage single-cell data identified two overlapping candidate genes: PDK4 and THBS1 (Fig. 2D and E). Both genes were significantly upregulated in PBMCs from non-survivors compared with survivors (P = 0.0055 and P = 0.0281, respectively) (Fig. 2F and G). Notably, receiver operating characteristic analysis showed that PDK4 had higher predictive performance for 28-day mortality (AUC = 0.88) than THBS1 (AUC = 0.78) (Fig. 2H). Moreover, upregulation of PDK4 in macrophages from patients with ACLF was more pronounced than that of THBS1 (PDK4: $\log_2$FC = 1.36; THBS1: $\log_2$FC = 1.10). Therefore, PDK4 was selected for further investigation.

In an independent validation cohort composed of newly

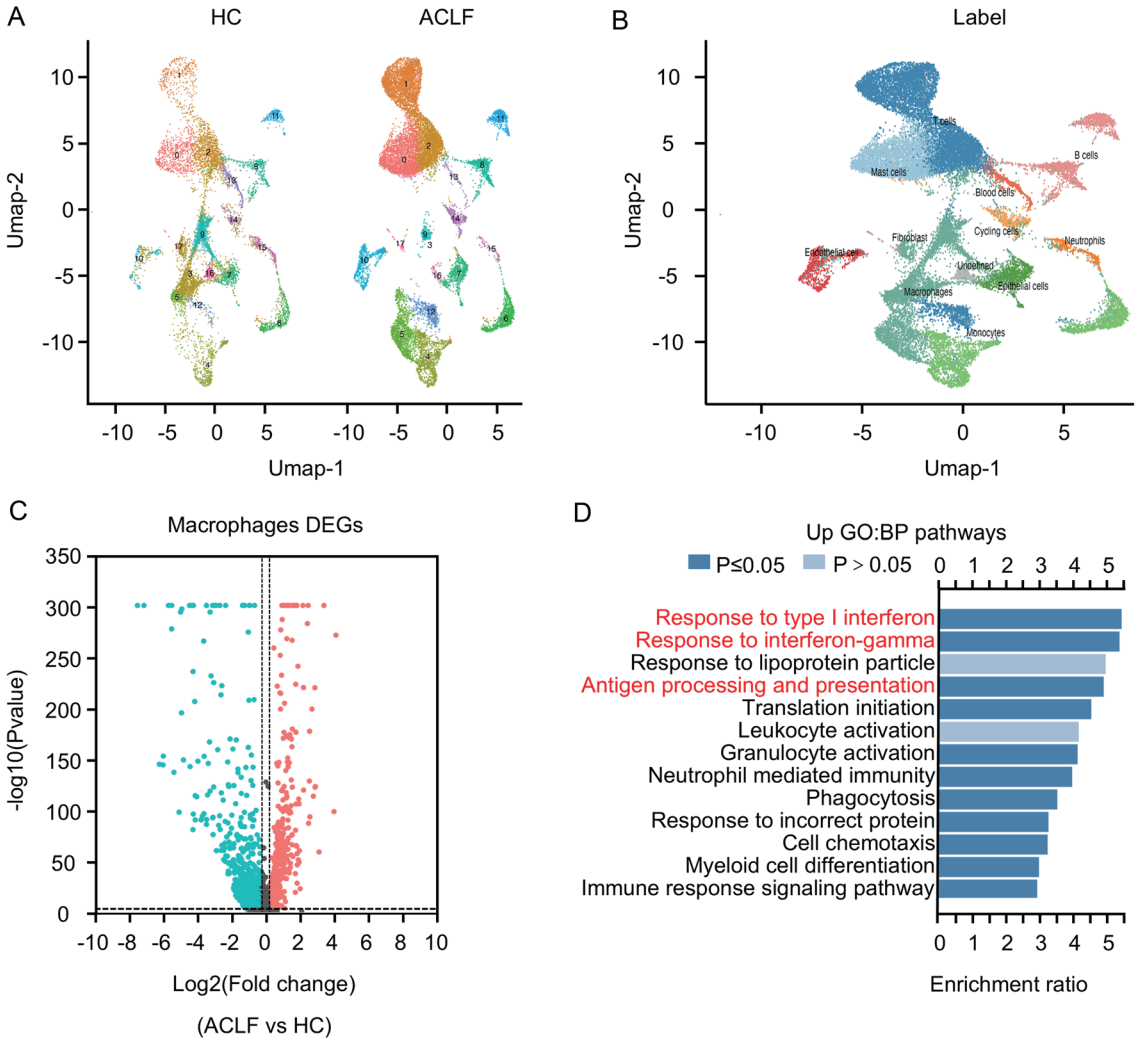

Fig. 1. Single-cell transcriptomic profiling of liver macrophages from patients with ACLF and HCs. (A, B) UMAP visualization of cell clustering and annotation based on canonical marker gene expression in liver tissue samples from five ACLF patients and three HCs. (C) Volcano plot showing DEGs in macrophages from ACLF versus HC samples. Genes with $|\log_2$ fold change$| > 0.25$ and $P < 0.05$ were considered statistically significant. Upregulated genes are shown in red, downregulated genes in cyan. (D) GO enrichment analysis for upregulated genes. Enriched pathways with FDR < 0.05 were considered significant. ACLF, acute-on-chronic liver failure; HC(s), healthy control(s); GO, Gene Ontology; FDR, false discovery rate.

collected clinical PBMC samples, RT-qPCR analysis further confirmed that PDK4 mRNA expression was significantly upregulated in PBMCs from patients with ACLF compared with HCs ($P = 0.0028$) (Fig. 2I). Further analysis showed that its expression level was significantly positively correlated with MELD scores ($R^2 = 0.7932$, $P < 0.0001$) and COSSH-ACLF II scores ($R^2 = 0.6057$, $P < 0.0001$) (Fig. 2J). Consistently, immunohistochemical and multiplex fluorescence staining of liver tissues revealed a marked increase in $CD68^+CD86^+$ M1-like macrophage infiltration in patients with ACLF. Notably, PDK4 expression was prominently upregulated in these M1-like macrophages (Fig. 2K). Collectively, these results suggest that PDK4 is a key gene involved in ACLF pathogenesis and progression, potentially acting by modulating macrophage phenotypes.

PDK4 is highly expressed in M1 macrophages under ACLF conditions both in vivo and in vitro

To investigate its role in macrophage immune function during ACLF, we first assessed PDK4 expression in *in vivo* mouse models of ACLF. RT-qPCR analysis showed that PDK4 expression was significantly increased in PBMCs and liver tissues from ACLF mice compared with HCs ($P = 0.0015$ and $P < 0.0001$, respectively) (Fig. 3A). In peritoneal macrophages isolated from ACLF mice, expression of CD86, a classical marker of M1 polarization, was significantly elevated, and PDK4 expression was also markedly upregulated in these macrophages ($P = 0.0005$ and $P = 0.0002$, respectively) (Fig. 3B).

We next examined whether PDK4 expression was induced during M1 macrophage polarization *in vitro*. Stimulation of THP-1 macrophages with LPS/IFN-γ, as well as LPS treatment of RAW264.7 cells, produced a time-dependent increase in CD86 expression, confirming successful M1 polarization. Concurrently, PDK4 expression progressively increased over time under both conditions (Fig. 3C–F). Subsequently, we observed increased phosphorylation of the PDK4 downstream substrate PDHE1α (Supplementary Fig. 1A and

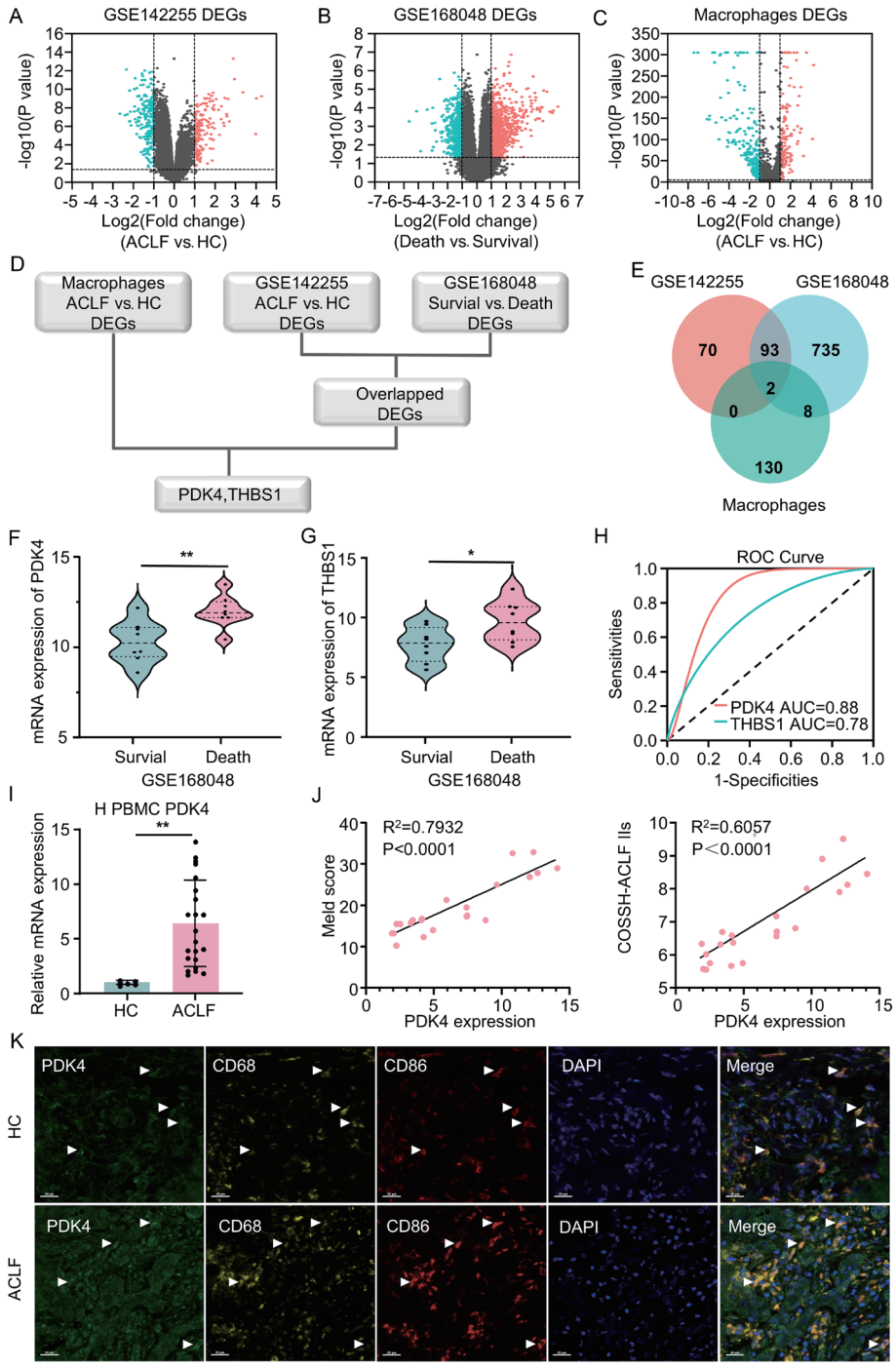

Fig. 2. Multi-dataset analysis of gene expression in ACLF. (A) Volcano plot of DEGs in whole blood between ACLF patients (n = 17) and HCs (n = 7) in the GSE142255 dataset, with $|\log_2 FC| > 1$ and $P < 0.05$. Upregulated and downregulated genes are shown in red and cyan, respectively. (B) Volcano plot of DEGs in PBMCs between 28-day non-survivors (n = 8) and survivors (n = 8) in the GSE168048 dataset, using the same thresholds as in (A). (C) Volcano plot of DEGs in liver macrophages between ACLF patients (n = 7) and HCs (n = 3) based on scRNA-seq data (PRJNA913603), with $|\log_2 FC| > 1$ and $P < 0.05$. (D) Flowchart of the integrated analysis of DEGs from the three datasets. (E) Venn diagram showing the intersection of DEGs identified in analyses (A), (B), and (C). (F, G) Expression levels of PDK4 (F) and THBS1 (G) in 28-day non-survivors (n = 8) versus survivors (n = 8) in the GSE168048 cohort. Data are presented as mean ± SD. Statistical significance was assessed using an unpaired Student's t-test. (H) ROC curves of PDK4 and THBS1 from the GSE168048 dataset for predicting 28-day mortality in ACLF patients (n = 16). (I) RT-qPCR analysis of PDK4 mRNA levels in PBMCs from ACLF patients (n = 22) and HCs (n = 6). Data are presented as mean ± SD. Statistical significance was assessed using an unpaired Student's t-test. (J) Correlation analysis between PDK4 expression levels in PBMCs and MELD or COSSH-ACLF II scores in patients with ACLF (n = 22). Spearman's rank correlation coefficient was used to assess associations. (K) Multiplex immunofluorescence staining of PDK4, CD68, and CD86 in liver tissues from ACLF patients. $^*P < 0.05$, $^{**}P < 0.01$. ACLF, acute-on-chronic liver failure; DEGs, differentially expressed genes; HCs, healthy controls; scRNA-seq, single-cell RNA sequencing; PBMCs, peripheral blood mononuclear cells; MELD, Model for End-Stage Liver Disease; COSSH-ACLF II, Chinese Group on the Study of Severe Hepatitis B-ACLF II; ROC, receiver operating characteristic; AUC, area under the curve.

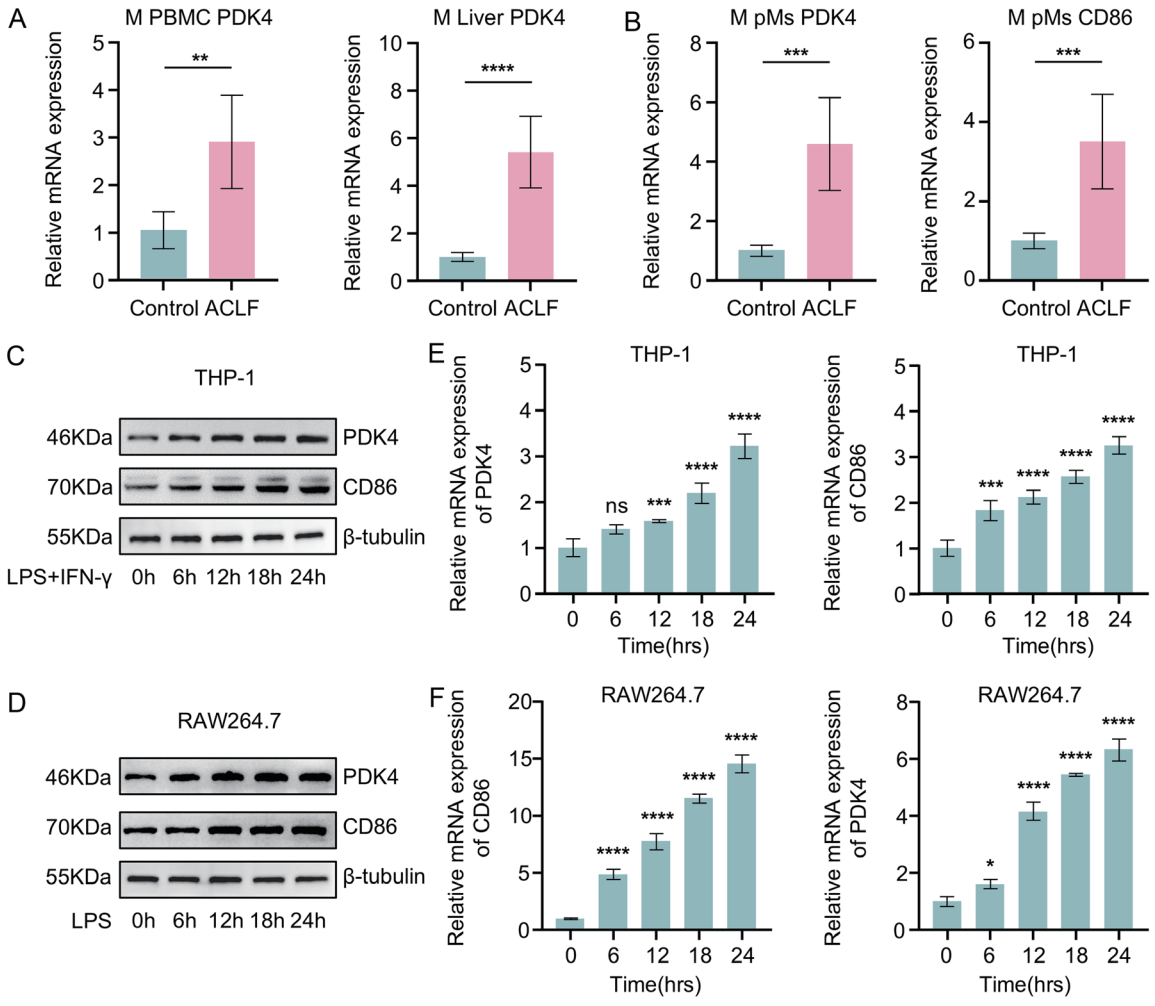

Fig. 3. Analysis of PDK4 expression in ACLF-related macrophage polarization models. (A) PDK4 mRNA expression levels in PBMCs and liver tissues from control (n = 6 per group) and ACLF (n = 6 per group) mice. (B) mRNA expression of CD86 and PDK4 in PMs isolated from control (n = 6 per group) and ACLF (n = 6 per group) mice. (C-F) CD86 and PDK4 expression in THP-1 macrophages and RAW264.7 cells after induction of M1 polarization (n = 3). Data are presented as mean ± SD. Statistical significance was determined by unpaired two-tailed Student's t-test (for comparisons between two groups) or one-way ANOVA (for comparisons among multiple groups). ns, $P > 0.05$, *$P < 0.05$, **$P < 0.01$, ***$P < 0.001$, ****$P < 0.0001$. PDK4, pyruvate dehydrogenase kinase 4; ACLF, acute-on-chronic liver failure; PBMCs, peripheral blood mononuclear cells; PMs, peritoneal macrophages; ns, not significant.

B), suggesting enhanced PDK4 enzymatic activity.

We further assessed PDK4 expression under M2-polarizing conditions. Treatment of THP-1 macrophages with IL-4 and IL-13, or stimulation of RAW264.7 cells with IL-4, successfully induced M2 polarization, as evidenced by increased CD206 expression (Supplementary Fig. 1C and D). Notably, PDK4 expression in M2-polarized macrophages did not differ significantly from unpolarized controls ($P = 0.4572$ and $P = 0.3153$, respectively) (Supplementary Fig. 1E and F).

These findings indicate that PDK4 upregulation is closely associated with M1 macrophage polarization during ACLF, consistently observed in both *in vivo* and *in vitro* models.

PDK4 overexpression promotes M1 polarization of macrophages in vitro

To elucidate the role of PDK4 in macrophage polarization, THP-1 macrophages were transfected with an OE-PDK4 or an OE-EV. Western blot analysis confirmed that PDK4 protein expression was significantly increased in OE-PDK4 THP-1 macrophages compared with OE-EV controls ($P = 0.0003$) (Fig. 4A).

Following transfection, OE-PDK4 and OE-EV THP-1 macrophages were stimulated with LPS/IFN-γ to induce M1 polarization. Western blot analysis showed that PDK4 overexpression markedly increased the M1 macrophage markers CD86 and iNOS relative to the OE-EV group (Fig. 4B). Flow cytometry further showed that the proportion of $CD86^+$ cells increased from 33.4% in the OE-EV group to 54.8% in the OE-PDK4 group ($P < 0.0001$) (Fig. 4C). Immunofluorescence staining also revealed significantly higher CD86 fluorescence intensity in the OE-PDK4 group compared with controls ($P = 0.0024$) (Fig. 4D), indicating that PDK4 overexpression promotes M1 polarization. To assess the functional consequences of PDK4 overexpression, the expression and secretion of pro-inflammatory cytokines were evaluated. RT-qPCR analysis revealed that the mRNA levels of IL-6 and TNF-α were significantly upregulated in OE-PDK4 macrophages compared with controls upon LPS/IFN-γ stimulation ($P = 0.0011$ and $P = 0.0008$, respectively) (Fig. 4E). In line with these findings, ELISA demonstrated that the secretion levels of IL-6 and

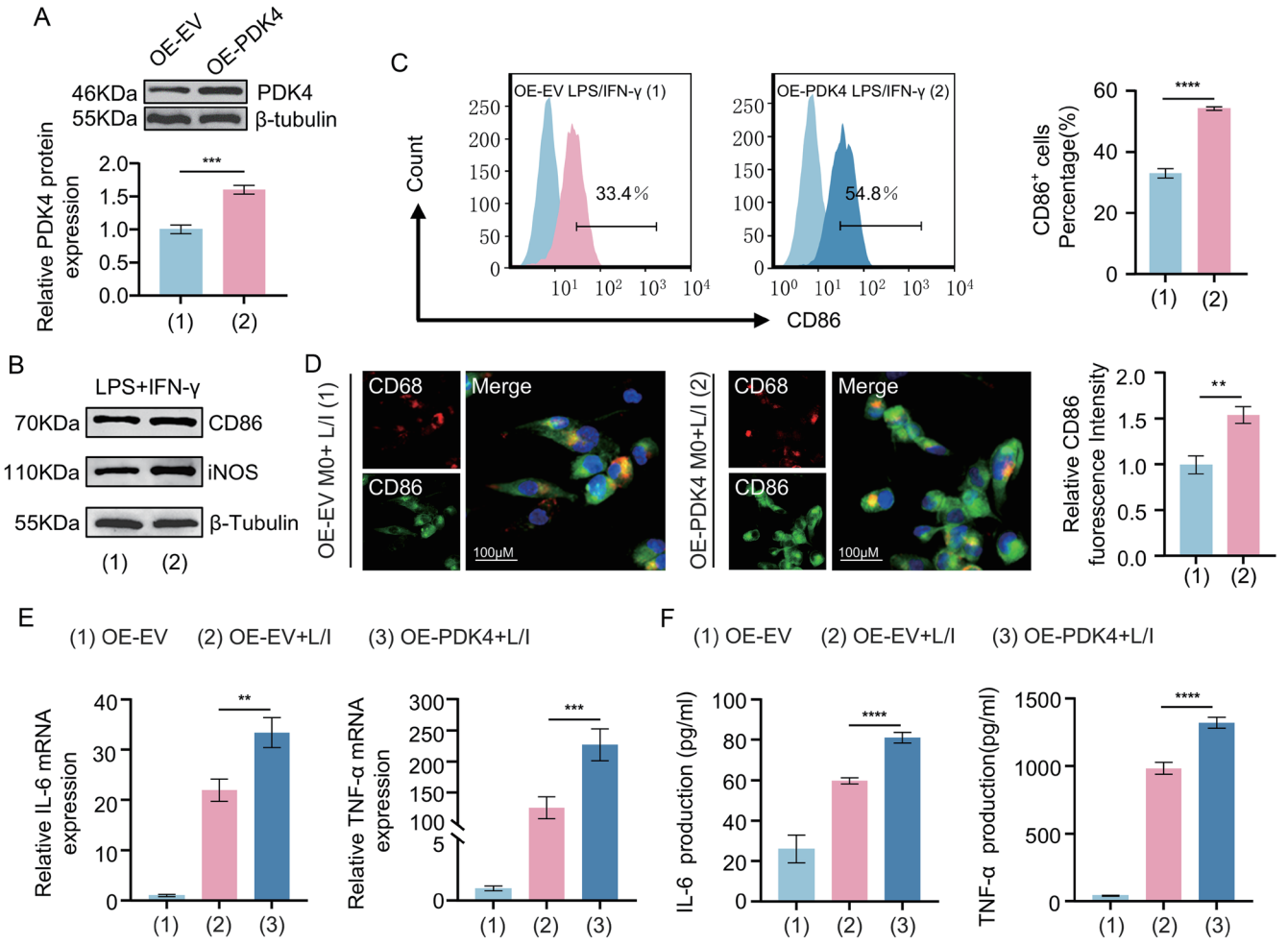

Fig. 4. Effects of PDK4 overexpression on M1 polarization markers in THP-1 macrophages. (A) PDK4 expression was assessed by Western blot in THP-1 macrophages transfected with PDK4 overexpression plasmid (OE-PDK4) or empty vector (OE-EV). (B) Protein levels of the M1 markers CD86 and iNOS were analyzed by Western blot. (C) The proportion of $CD86^+$ cells was determined by flow cytometry. (D) CD68 (red) and CD86 (green) expression was visualized by immunofluorescence staining; nuclei were counterstained with DAPI (blue); scale bar = 100 μm. (E) mRNA expression of IL-6 and TNF-α was measured by RT-qPCR. (F) Secreted levels of IL-6 and TNF-α in the supernatant were quantified by ELISA. Data are presented as mean ± SD (n = 3). Statistical significance was determined by unpaired two-tailed Student's t-test (for comparisons between two groups) or one-way ANOVA (for comparisons among multiple groups). $^{**}P < 0.01$, $^{***}P < 0.001$, $^{****}P < 0.0001$. OE-PDK4, PDK4 overexpression plasmid; OE-EV, overexpression empty vector; LPS, lipopolysaccharide; IFN-γ, interferon-gamma; CD86, cluster of differentiation 86; iNOS, inducible nitric oxide synthase; IL-6, interleukin-6; TNF-α, tumor necrosis factor-alpha.

TNF-α were also markedly increased in the OE-PDK4 group ($P < 0.0001$ for each) (Fig. 4F).

Collectively, these findings indicate that PDK4 overexpression promotes M1 polarization of macrophages and enhances expression and secretion of the pro-inflammatory cytokines IL-6 and TNF-α *in vitro*.

Inhibition of PDK4 attenuates M1-like polarization of macrophages and alleviates LO2 cell injury

To explore the role of PDK4 inhibition in macrophage polarization, we first assessed the cytotoxicity of a PDK4-IN in THP-1 macrophages using a CCK-8 assay. PDK4-IN at concentrations below 10 μM had no significant effect on cell viability ($P = 0.1508$) (Fig. 5A). Based on these results, low (0.625 μM), medium (2.5 μM), and high (5 μM) concentrations were selected for subsequent experiments. Western blot analysis showed that PDK4-IN pretreatment reduced the M1 macrophage markers CD86 and iNOS in a dose-dependent manner after LPS and IFN-γ stimulation, with the most significant suppression at the high concentration ($P < 0.0001$ and $P = 0.0001$, respectively) (Fig. 5B, Supplementary Fig. 2A). To determine the minimal effective concentration for M1 polarization inhibition, we tested lower doses (0.312 μM and 0.156 μM). CD86 expression was unchanged at these concentrations ($P = 0.9973$ and $P = 0.4466$, respectively) (Supplementary Fig. 2B), indicating that 0.625 μM is the minimal effective concentration.

Flow cytometry further confirmed that the proportion of $CD86^+$ macrophages was significantly decreased after PDK4-IN pretreatment (5 μM, $P = 0.0005$) (Fig. 5C). Consistently, immunofluorescence staining showed reduced CD86 in macrophages treated with PDK4-IN (5 μM), with a significant decrease in relative fluorescence intensity ($P = 0.0011$) (Fig. 5D). In addition, RT-qPCR analysis showed that PDK4-IN pretreatment downregulated IL-6 and TNF-α mRNA in a concentration-dependent manner, with the most significant suppression at the high concentration ($P < 0.0001$ for each) (Fig. 5E). ELISA confirmed that PDK4-IN pretreatment signif-

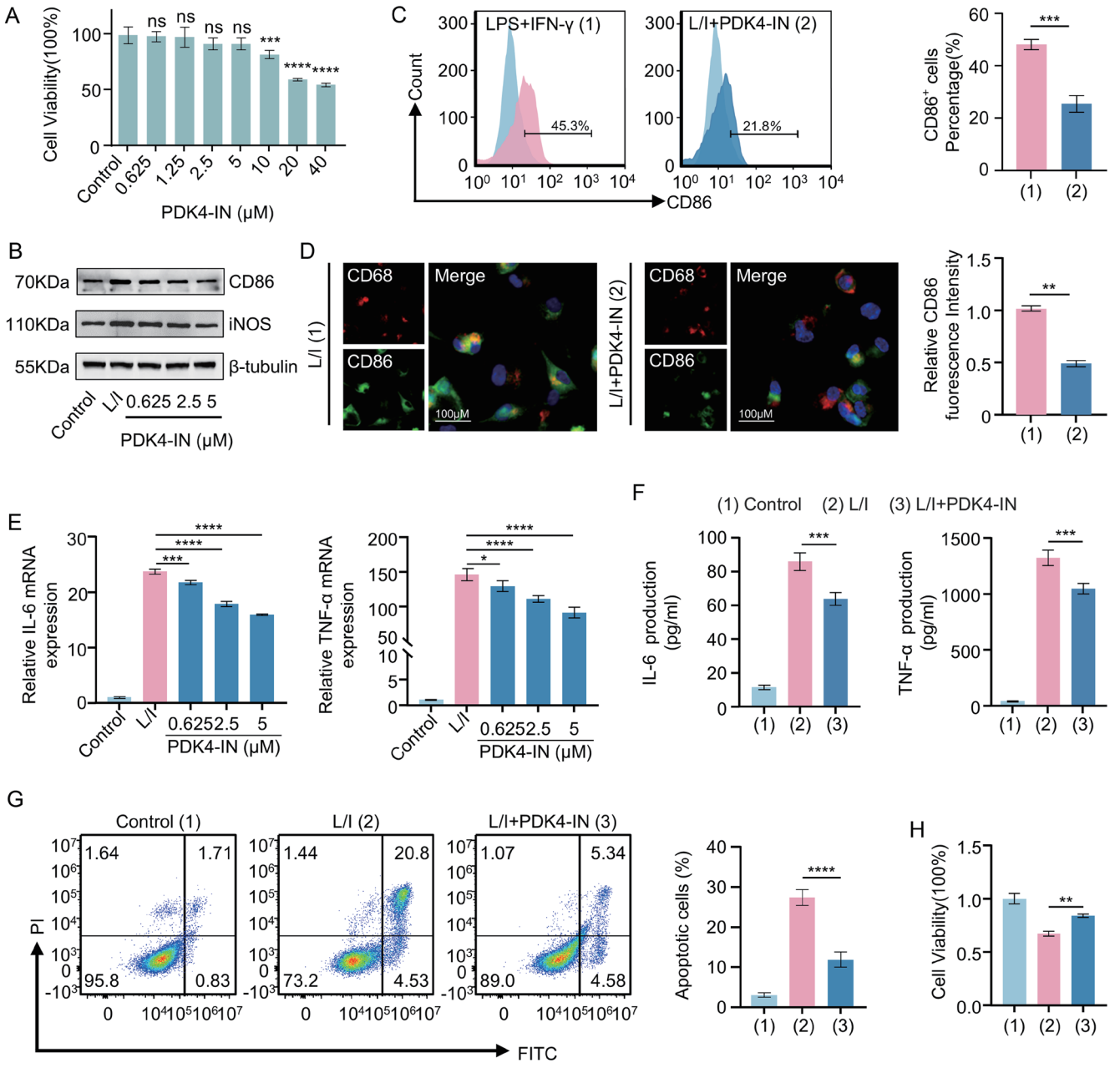

Fig. 5. Effects of PDK4 inhibition on M1 polarization in THP-1 macrophages and hepatocyte injury. (A) Cell viability of THP-1 macrophages treated with increasing concentrations of PDK4-IN (0–40 μM) for 24 h was assessed by CCK-8 assay. (B) Protein levels of the M1 markers CD86 and iNOS were analyzed by Western blot. (C) The proportion of $CD86^+$ cells was determined by flow cytometry. (D) CD68 (red) and CD86 (green) expression was visualized by immunofluorescence staining; nuclei were counterstained with DAPI (blue); scale bar = 100 μm. Quantification of fluorescence intensity is shown on the right. (E) mRNA expression of IL-6 and TNF-α was measured by RT-qPCR. (F) Secreted levels of IL-6 and TNF-α in the supernatant were quantified by ELISA. (G) Flow cytometric analysis of apoptosis in LO2 cells cultured with conditioned media derived from macrophages. (H) CCK-8 assay of viability in LO2 cells cultured with conditioned media derived from macrophages. Data are presented as mean ± SD (n = 3). Statistical significance was determined by unpaired two-tailed Student's t-test (for comparisons between two groups) or one-way ANOVA (for comparisons among multiple groups). ns, $P > 0.05$, $^*P < 0.05$, $^{**}P < 0.01$, $^{***}P < 0.001$, $^{****}P < 0.0001$. PDK4-IN, pyruvate dehydrogenase kinase 4 inhibitor; CCK-8, Cell Counting Kit-8; CD86, cluster of differentiation 86; iNOS, inducible nitric oxide synthase; IL-6, interleukin-6; TNF-α, tumor necrosis factor-alpha; LPS, lipopolysaccharide; IFN-γ, interferon-gamma; DAPI, 4′,6-diamidino-2-phenylindole; ns, not significant.

icantly reduced secretion of IL-6 and TNF-α in supernatants of stimulated macrophages ($P = 0.0007$ and $P = 0.0008$, respectively) (Fig. 5F).

Importantly, we found that conditioned media from PDK4-IN-pretreated macrophages reduced LO2 hepatocyte apoptosis ($P < 0.0001$) (Fig. 5G) and increased cell viability ($P = 0.0012$) (Fig. 5H) compared with media from macrophages treated with LPS/IFN-γ alone.

PDK4 promotes macrophage M1 polarization via STAT1-dependent signaling

To investigate downstream mechanisms by which PDK4

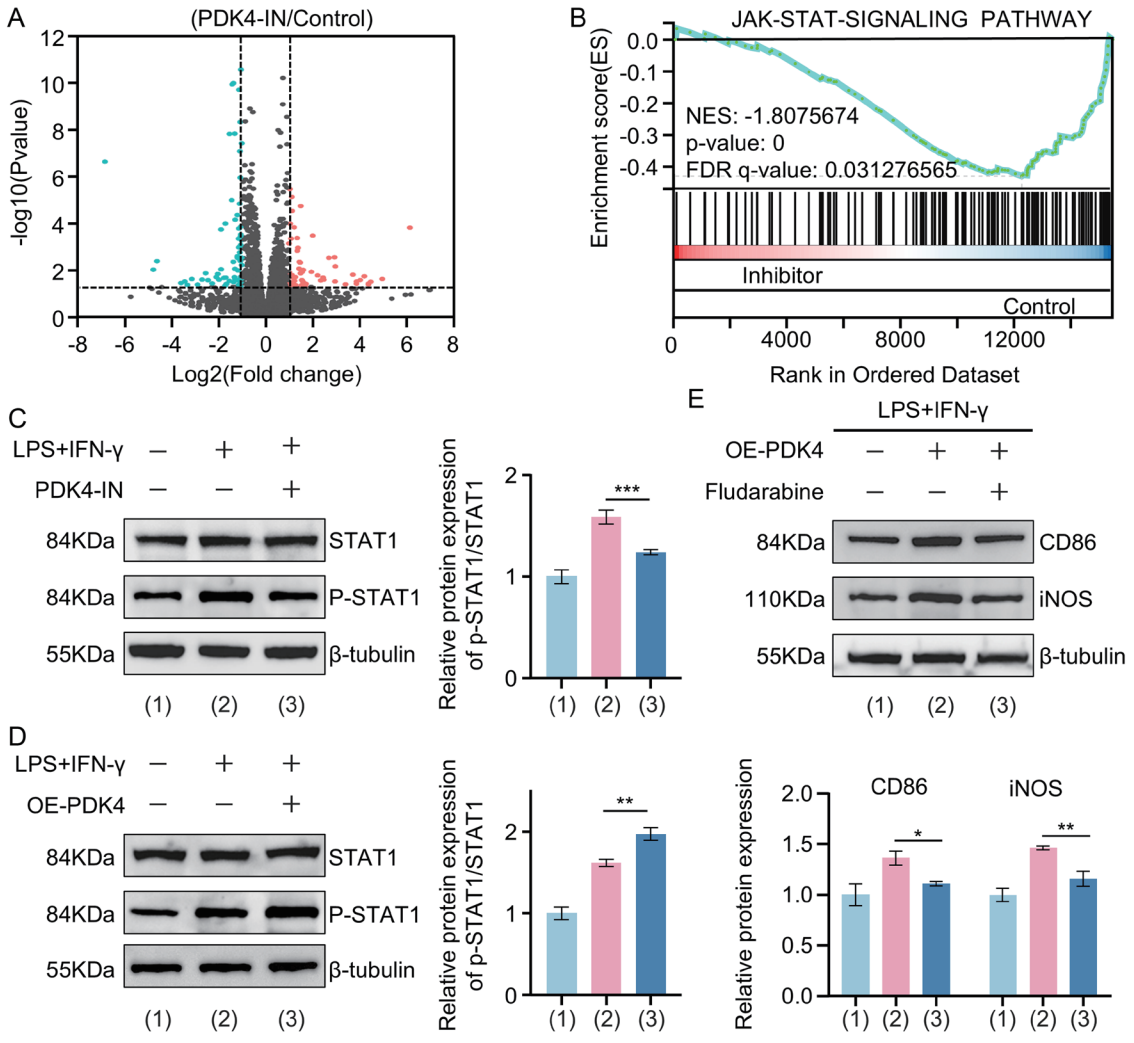

Fig. 6. Effects of PDK4 inhibition or overexpression on STAT1 phosphorylation and M1 polarization in macrophages. (A) Volcano plot showing DEGs in macrophages stimulated with LPS/IFN-γ, with or without pretreatment with PDK4-IN. Upregulated genes are shown in red, downregulated genes in cyan. (B) GSEA of transcriptomic data. (C, D) Western blot analysis and quantification of total STAT1 and p-STAT1. Cells were pretreated with either PDK4-IN or PDK4 overexpression vector, followed by LPS/IFN-γ stimulation. (E) Western blot analysis and quantification of M1 polarization markers CD86 and iNOS under PDK4 overexpression in the presence or absence of the STAT1 inhibitor fludarabine. Data are presented as mean ± SD (n = 3). Statistical significance was determined by one-way ANOVA followed by Tukey's post hoc test. **P* < 0.05, ***P* < 0.01, ****P* < 0.001. +, with; -. without; PDK4, pyruvate dehydrogenase kinase 4; STAT1, signal transducer and activator of transcription 1; p-STAT1, phosphorylated STAT1; DEGs, differentially expressed genes; GSEA, gene set enrichment analysis; LPS, lipopolysaccharide; IFN-γ, interferon-gamma; CD86, cluster of differentiation 86; iNOS, inducible nitric oxide synthase.

regulates macrophage polarization, we performed transcriptome sequencing. The results showed that PDK4 inhibition significantly altered the gene expression profile of LPS/IFN-γ-stimulated THP-1 macrophages, identifying a total of 172 DEGs, including 46 upregulated and 126 downregulated genes (Q value < 0.05) (Fig. 6A). GSEA further showed that the JAK-STAT signaling pathway was significantly suppressed in the PDK4-IN group (NES = −1.8076, FDR q-value = 0.0313) (Fig. 6B).

Western blot analysis was performed to further validate the effect of PDK4 inhibition on STAT1 activation. Compared with control, LPS/IFN-γ stimulation markedly increased STAT1 phosphorylation, whereas PDK4-IN pretreatment significantly reduced this response (P = 0.0006) (Fig. 6C). Conversely, PDK4 overexpression further enhanced STAT1 phosphorylation after LPS/IFN-γ stimulation (P = 0.0013) (Fig. 6D).

To determine whether PDK4 promotes macrophage M1 polarization via STAT1, we examined expression of the M1 markers CD86 and iNOS. PDK4 overexpression significantly increased CD86 and iNOS protein levels, whereas treatment with the STAT1 inhibitor fludarabine effectively reversed these increases (P = 0.0110 and P = 0.0011, respectively) (Fig. 6E). These findings demonstrate that PDK4 facilitates macrophage M1-like polarization through increased STAT1 phosphorylation.

Inhibition of PDK4 attenuates hepatic injury in mice by suppressing macrophage M1 polarization

To investigate the role of PDK4 in the pathogenesis of ACLF, a mouse model was established by chronic administration of CCl_4 combined with acute stimulation by LPS/D-GalN. A PDK4-IN was given orally 8 h before acute stimulation (Fig. 7A). Gross examination and hematoxylin-eosin staining showed that livers from ACLF mice exhibited extensive hem-

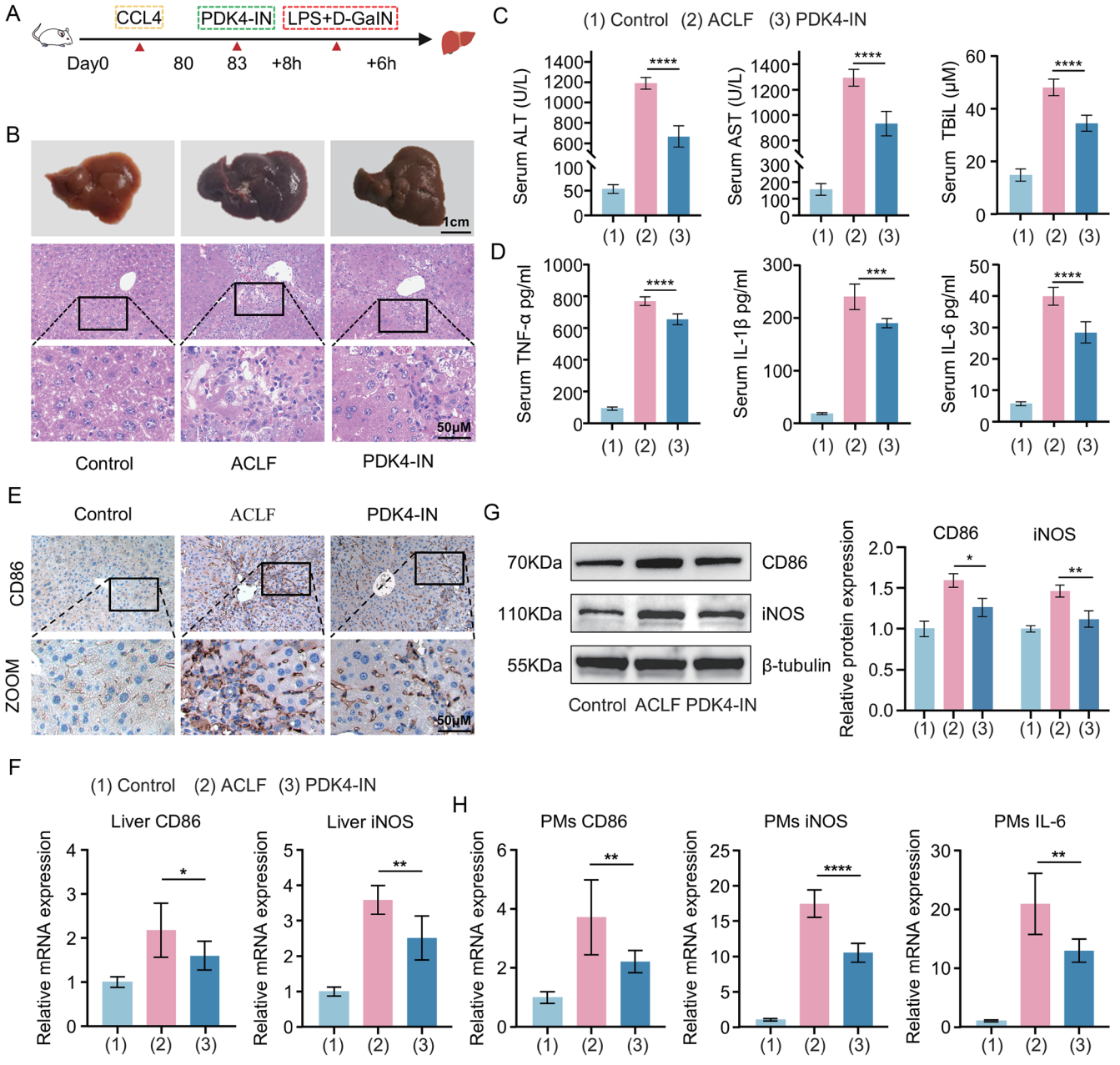

Fig. 7. Effects of PDK4 inhibition on hepatic injury and macrophage M1 polarization in mice with ACLF. (A) Schematic diagram of the experimental protocol. (B) Gross morphology and HE staining of liver tissues from control, ACLF, and PDK4-IN groups (n = 6 per group). Scale bars: 1 cm for gross morphology and 50 μm for HE-stained images. (C) Serum levels of ALT, AST, and TBIL. (D) Serum concentrations of TNF-α, IL-1β, and IL-6. (E) Immunohistochemical staining for CD86 in liver tissues. Scale bar = 50 μm. (F, G) Western blot and RT-qPCR analyses of CD86 and iNOS protein and mRNA expression levels in liver tissues. (H) RT-qPCR analysis of CD86, iNOS, and IL-6 mRNA levels in PMs. Data are presented as mean ± SD (n = 6 per group). Statistical significance was determined by one-way ANOVA followed by Tukey's post hoc test. **P* < 0.05, ***P* < 0.01, ****P* < 0.001, *****P* < 0.0001. ACLF, acute-on-chronic liver failure; PDK4, pyruvate dehydrogenase kinase 4; PDK4-IN, PDK4 inhibitor; PMs, peritoneal macrophages; ALT, alanine aminotransferase; AST, aspartate aminotransferase; TBIL, total bilirubin; TNF-α, tumor necrosis factor-alpha; IL-1β, interleukin-1 beta; IL-6, interleukin-6; iNOS, inducible nitric oxide synthase.

orrhage and necrosis with severely disrupted hepatic architecture. In contrast, PDK4-IN treatment markedly improved liver appearance and preserved tissue structure (Fig. 7B). Serum biochemical analysis showed that alanine aminotransferase, aspartate aminotransferase, and total bilirubin were significantly elevated in ACLF mice compared with controls, whereas PDK4-IN significantly reduced transaminases and bilirubin ($P < 0.0001$ for each) (Fig. 7C). Consistently, serum cytokine analysis indicated that TNF-α, IL-1β, and IL-6 were markedly increased in ACLF mice, and PDK4-IN significantly suppressed these cytokines ($P < 0.0001$, $P = 0.0004$, and $P < 0.0001$, respectively) (Fig. 7D).

Immunohistochemical analysis showed that the M1 macrophage marker CD86 was significantly upregulated in livers of ACLF mice compared with controls, whereas PDK4-IN treatment markedly reduced the area of positive staining

for this marker (Fig. 7E). Consistently, RT-qPCR analysis showed that PDK4-IN treatment significantly reduced mRNA expression of both CD86 and iNOS in livers of ACLF mice ($P = 0.0478$ and $P = 0.0011$, respectively) (Fig. 7F). Similarly, Western blot analysis revealed that CD86 and iNOS protein levels were also significantly decreased ($P = 0.0106$ and $P = 0.0025$, respectively) (Fig. 7G). In peritoneal macrophages, PDK4-IN also downregulated mRNA expression of CD86, iNOS, and IL-6 ($P = 0.0079$, $P < 0.0001$, and $P = 0.0012$, respectively) (Fig. 7H). Collectively, these results suggest that PDK4 inhibition attenuates liver injury and systemic inflammation in ACLF mice, at least in part, by suppressing macrophage M1 polarization.

Discussion

ACLF is a life-threatening clinical syndrome characterized by systemic inflammation and immune dysregulation, with a markedly high mortality rate.[34,35] Emerging evidence indicates that macrophage polarization plays a pivotal role in immune imbalance and disease progression during ACLF.[36,37] In this study, we identified PDK4 as a crucial modulator of macrophage function that contributes to the development and progression of ACLF.

Previous studies have shown that PDK4 is upregulated in various inflammatory diseases, such as sarcoidosis and septic cardiomyopathy, and its expression correlates with disease severity.[38,39] However, studies have also reported downregulated PDK4 expression in synovial cells from rheumatoid arthritis, suggesting that its function may be disease-specific.[40] Our study revealed that high PDK4 expression in PBMCs was significantly associated with poor clinical outcomes in patients with ACLF, suggesting that PDK4 may serve as a biomarker reflecting the extent of inflammation and disease progression, with prognostic value. Notably, PDK4 is not only upregulated in various inflammatory diseases but may also actively contribute to inflammation and disease progression by modulating immune cell function. PDK4 influences multiple immune cell types, including macrophages and T cells.[16,41] Specifically, PDK2 and PDK4 act as metabolic checkpoints of macrophage polarization. Genetic deletion or pharmacologic inhibition of these kinases significantly attenuated M1 polarization in high-fat diet–induced models of insulin resistance.[42] Moreover, advanced glycation end products promoted M1 macrophage polarization by activating the HIF-1α/PDK4 signaling pathway.[43] Consistently, our findings showed that PDK4 was markedly upregulated under M1-polarizing conditions, highlighting its critical role in macrophage functional programming. PDK4 overexpression led to a pronounced increase in M1-associated markers, including CD86 and iNOS, and enhanced secretion of key pro-inflammatory cytokines such as TNF-α and IL-6. Persistent elevation of these cytokines is closely linked to immune dysregulation, exacerbated hepatic injury, and multiorgan failure, and their circulating levels correlate positively with poor short-term prognosis, serving as predictors of early mortality.[44–46] Conversely, pharmacologic inhibition of PDK4 significantly suppressed M1 polarization and reduced production of pro-inflammatory mediators, highlighting its essential role in sustaining the M1 phenotype and amplifying the inflammatory cascade.

Inhibition of macrophage M1 polarization has been recognized as an effective strategy to alleviate liver injury. Previous studies showed that mesenchymal stem cell therapy could alleviate liver inflammation and injury by suppressing M1 polarization.[47] More recently, a traditional Chinese herbal formulation, Chishao-Fuzi, was reported to improve liver function, coagulation abnormalities, and histopathologic damage in ACLF rats through a similar mechanism.[36] In our *in vitro* experiments, supernatants from conventional M1 macrophages significantly induced injury in LO2 hepatocytes, whereas supernatants from PDK4-inhibited M1 macrophages showed markedly reduced cytotoxicity, suggesting that PDK4 inhibition could attenuate M1-mediated hepatocellular injury. *In vivo*, treatment with a PDK4 inhibitor in ACLF mice reduced intrahepatic infiltration of M1 macrophages and ameliorated inflammatory responses and histopathologic alterations, further supporting the therapeutic potential of targeting PDK4 to inhibit M1 macrophage polarization in ACLF.

Previous studies have established that STAT1 activation is a key mechanism driving macrophage polarization toward the pro-inflammatory M1 phenotype.[11,48] Our study found that PDK4 overexpression significantly promoted M1 polarization and enhanced STAT1 phosphorylation, whereas PDK4 inhibition concurrently reduced STAT1 phosphorylation and the M1 polarization capacity of macrophages. Although PDK4 was previously thought to drive M1 polarization primarily through enhanced glycolysis and metabolic reprogramming, our findings reveal that it also facilitates M1 polarization by activating the STAT1 signaling pathway, suggesting a novel regulatory mechanism and providing new insights into its immunomodulatory function.

Notably, the precise mechanism by which PDK4 regulates STAT1 remains to be defined. As a metabolism-associated enzyme, PDK4 promotes glycolysis, suppresses oxidative phosphorylation, and induces mitochondrial dysfunction. Based on current evidence, we hypothesize that PDK4 may indirectly activate STAT1 through enhanced glycolysis and the consequent burst of reactive oxygen species, a notion supported by multiple studies.[49,50] Moreover, we cannot exclude the possibility that PDK4 directly modulates STAT1 activity via non-metabolic mechanisms, such as protein–protein interactions.

From a clinical translation perspective, targeting PDK4 holds substantial therapeutic potential. By specifically inhibiting M1 polarization and the ensuing cytokine storm, this strategy may markedly attenuate hepatocellular injury and systemic inflammation, as reflected by reduced transaminases, bilirubin, and inflammatory markers such as IL-6. Intervening in this pivotal pathway is also expected to mitigate the progression of multiple organ failure, thereby potentially improving short-term survival. Future studies should prioritize the development of liver-targeted nanoparticle delivery systems to enhance drug specificity and explore combination strategies with existing treatments, such as artificial liver support systems. Further validation of this pathway across ACLF models of diverse etiologies will facilitate clinical translation.

We acknowledge several limitations. First, given the multifaceted roles of PDK4 in metabolic and inflammatory regulation, its effects may not be confined to macrophages and could involve non-macrophage-mediated mechanisms that warrant investigation. Second, although this study focused on the correlation between PDK4 and STAT1 signaling, the causal molecular mechanisms remain incompletely defined and require further validation through in-depth experiments. Finally, although regulation of STAT1 signaling by PDK4 has not yet been validated in animal models, the significant immunomodulatory effects observed in the ACLF model suggest that PDK4 represents a promising therapeutic target in ACLF and merits rigorous exploration.

Conclusions

This study demonstrates that PDK4 promotes M1 macrophage

polarization in ACLF by activating STAT1 signaling, exacerbating hepatocellular injury and systemic inflammation. Our work addresses a critical knowledge gap by identifying the PDK4–STAT1 axis as a pivotal immunologic mechanism in ACLF pathogenesis and supports its therapeutic targeting. Limitations involve potential non-macrophage effects of PDK4 and unvalidated mechanistic and *in vivo* links to STAT1 signaling. Further studies should validate this pathway across diverse ACLF models and advance the development of PDK4-targeted inhibitors for clinical translation.

Acknowledgments

We thank all patients recruited in this study for their participation.

Funding

This study was supported by the Central Government-Guided Local Science and Technology Development Fund Project (Science and Technology Innovation Base Project) (236Z7749G); Hebei Provincial Precision Medicine Innovation and Development Joint Fund Incubation Project (H2025206547); and Hebei Provincial Basic Research Special Youth Science Fund Project (H2025206274).

Conflict of interest

The authors have no conflict of interests related to this publication.

Author contributions

Study concept and design (SD, LM, CZ), acquisition of data, experiments, analysis and interpretation of data (SD, LM, RG, XL, YX), drafting of the manuscript (SD, CZ), and revision of the writing and project supervision (CZ, CS). All authors made significant contributions to the study and approved the final manuscript.

Ethical statement

All animal experiments were approved by the Medical Ethics Committee of the Third Hospital of Hebei Medical University (Approval number: Z2024-036-2). All animals received human care. The study involving human participants was ethically reviewed and approved by the Ethics Committee of the Third Hospital of Hebei Medical University (Approval number: K2024-052-1) and was conducted in accordance with the principles of the Declaration of Helsinki (as revised in 2024). Written informed consent was obtained from all participants prior to their involvement in the study.

Data sharing statement

The datasets used in the study are available from the corresponding author upon reasonable request.

References

[1] Kulkarni AV, Sarin SK. Acute-on-chronic liver failure - steps towards harmonization of the definition!. J Hepatol 2024;81(2):360–366. doi:10.1016/j.jhep.2024.03.036, PMID:38554849.
[2] Choudhury A, Kulkarni AV, Arora V, Soin AS, Dokmeci AK, Chowdhury A, *et al*. Acute-on-chronic liver failure (ACLF): the 'Kyoto Consensus'-steps from Asia. Hepatol Int 2025;19(1):1–69. doi:10.1007/s12072-024-10773-4, PMID:39961976.
[3] European Association for the Study of the Liver. EASL Clinical Practice Guidelines on acute-on-chronic liver failure. J Hepatol 2023;79(2):461–491. doi:10.1016/j.jhep.2023.04.021, PMID:37364789.
[4] Mezzano G, Juanola A, Cardenas A, Mezey E, Hamilton JP, Pose E, *et al*. Global burden of disease: acute-on-chronic liver failure, a systematic review and meta-analysis. Gut 2022;71(1):148–155. doi:10.1136/gutjnl-2020-322161, PMID:33436495.
[5] van Hoek B. Defining the Value of Extracorporeal Liver Support in Acute and Acute-on-chronic Liver Failure. J Clin Transl Hepatol 2023;11(3):517–520. doi:10.14218/JCTH.2022.00025, PMID:36969899.
[6] An R, Wang JL. Acute liver failure: A clinically severe syndrome characterized by intricate mechanisms. World J Hepatol 2024;16(7):1067–1069. doi:10.4254/wjh.v16.i7.1067, PMID:39086537.
[7] Engelmann C, Zhang IW, Clària J. Mechanisms of immunity in acutely decompensated cirrhosis and acute-on-chronic liver failure. Liver Int 2025;45(3):e15644. doi:10.1111/liv.15644, PMID:37365995.
[8] Yunna C, Mengru H, Lei W, Weidong C. Macrophage M1/M2 polarization. Eur J Pharmacol 2020;877:173090. doi:10.1016/j.ejphar.2020.173090, PMID:32234529.
[9] Xu Y, Wang J, Ren H, Dai H, Zhou Y, Ren X, *et al*. Human endoderm stem cells reverse inflammation-related acute liver failure through cystatin SN-mediated inhibition of interferon signaling. Cell Res 2023;33(2):147–164. doi:10.1038/s41422-022-00760-5, PMID:36670290.
[10] An R, Zhu Z, Chen Y, Guan W, Wang J, Ren H. MSCs Suppress Macrophage Necroptosis and Foster Liver Regeneration by Modulating SP1/SK1 Axis in Treating Acute Severe Autoimmune Hepatitis. Adv Sci (Weinh) 2025;12(12):e2408974. doi:10.1002/advs.202408974, PMID:39899606.
[11] Sica A, Mantovani A. Macrophage plasticity and polarization: in vivo veritas. J Clin Invest 2012;122(3):787–795. doi:10.1172/JCI59643, PMID:22378047.
[12] Dąbrowska A, Wilczyński B, Mastalerz J, Kucharczyk J, Kulbacka J, Szewczyk A, *et al*. The Impact of Liver Failure on the Immune System. Int J Mol Sci 2024;25(17):9522. doi:10.3390/ijms25179522, PMID:39273468.
[13] Atas E, Oberhuber M, Kenner L. The Implications of PDK1-4 on Tumor Energy Metabolism, Aggressiveness and Therapy Resistance. Front Oncol 2020;10:583217. doi:10.3389/fonc.2020.583217, PMID:33384955.
[14] Roche TE, Hiromasa Y. Pyruvate dehydrogenase kinase regulatory mechanisms and inhibition in treating diabetes, heart ischemia, and cancer. Cell Mol Life Sci 2007;64(7-8):830–849. doi:10.1007/s00018-007-6380-z, PMID:17310282.
[15] Jeon JH, Thoudam T, Choi EJ, Kim MJ, Harris RA, Lee IK. Loss of metabolic flexibility as a result of overexpression of pyruvate dehydrogenase kinases in muscle, liver and the immune system: Therapeutic targets in metabolic diseases. J Diabetes Investig 2021;12(1):21–31. doi:10.1111/jdi.13345, PMID:32628351.
[16] Lee H, Jeon JH, Lee YJ, Kim MJ, Kwon WH, Chanda D, *et al*. Inhibition of Pyruvate Dehydrogenase Kinase 4 in CD4(+) T Cells Ameliorates Intestinal Inflammation. Cell Mol Gastroenterol Hepatol 2023;15(2):439–461. doi:10.1016/j.jcmgh.2022.09.016, PMID:36229019.
[17] Hao Y, Hao S, Andersen-Nissen E, Mauck WM 3rd, Zheng S, Butler A, *et al*. Integrated analysis of multimodal single-cell data. Cell 2021;184(13):3573–3587.e29. doi:10.1016/j.cell.2021.04.048, PMID:34062119.
[18] Liao Y, Wang J, Jaehnig EJ, Shi Z, Zhang B. WebGestalt 2019: gene set analysis toolkit with revamped UIs and APIs. Nucleic Acids Res 2019;47(W1):W199–W205. doi:10.1093/nar/gkz401, PMID:31114916.
[19] Zhai H, Zhang J, Shang D, Zhu C, Xiang X. The progress to establish optimal animal models for the study of acute-on-chronic liver failure. Front Med (Lausanne) 2023;10:1087274. doi:10.3389/fmed.2023.1087274, PMID:36844207.
[20] Lee D, Pagire HS, Pagire SH, Bae EJ, Dighe M, Kim M, *et al*. Discovery of Novel Pyruvate Dehydrogenase Kinase 4 Inhibitors for Potential Oral Treatment of Metabolic Diseases. J Med Chem 2019;62(2):575–588. doi:10.1021/acs.jmedchem.8b01168, PMID:30623649.
[21] Zhao HY, Zhang YY, Xing T, Tang SQ, Wen Q, Lyu ZS, *et al*. M2 macrophages, but not M1 macrophages, support megakaryopoiesis by upregulating PI3K-AKT pathway activity. Signal Transduct Target Ther 2021;6(1):234. doi:10.1038/s41392-021-00627-y, PMID:34140465.
[22] Zhao T, Zhong G, Wang Y, Cao R, Song S, Li Y, *et al*. Pregnane X Receptor Activation in Liver Macrophages Protects against Endotoxin-Induced Liver Injury. Adv Sci (Weinh) 2024;11(19):e2308771. doi:10.1002/advs.202308771, PMID:38477509.
[23] Huang W, Hong Y, He W, Jiang L, Deng W, Peng B, *et al*. Cavin-1 promotes M2 macrophages/microglia polarization via SOCS3. Inflamm Res 2022;71(4):397–407. doi:10.1007/s00011-022-01550-w, PMID:35275225.
[24] Yang B, Luo W, Wang M, Tang Y, Zhu W, Jin L, *et al*. Macrophage-specific MyD88 deletion and pharmacological inhibition prevents liver damage in non-alcoholic fatty liver disease via reducing inflammatory response. Biochim Biophys Acta Mol Basis Dis 2022;1868(10):166480. doi:10.1016/j.bbadis.2022.166480, PMID:35811033.
[25] Livak KJ, Schmittgen TD. Analysis of relative gene expression data using real-time quantitative PCR and the 2(-Delta Delta C(T)) Method. Methods 2001;25(4):402–408. doi:10.1006/meth.2001.1262, PMID:11846609.
[26] Song M, Ma L, Shen C, Liu W, Zhang P, Bi R, *et al*. FGD5-AS1/miR-5590-3p/PINK1 induces Lenvatinib resistance in hepatocellular carcinoma. Cell Signal 2023;111:110828. doi:10.1016/j.cellsig.2023.110828, PMID:37517671.
[27] Chen S, Tao L, Zhu F, Wang Z, Zhuang Q, Li Y, *et al*. BushenHuoxue decoction suppresses M1 macrophage polarization and prevents LPS induced inflammatory bone loss by activating AMPK pathway. Heliyon 2023;9(5):e15583. doi:10.1016/j.heliyon.2023.e15583, PMID:37153438.
[28] Ye Q, Luo F, Yan T. Transcription factor KLF4 regulated STAT1 to promote M1 polarization of macrophages in rheumatoid arthritis. Aging (Albany NY) 2022;14(14):5669–5680. doi:10.18632/aging.204128, PMID:35748767.
[29] Stack EC, Wang C, Roman KA, Hoyt CC. Multiplexed immunohistochemis-

try, imaging, and quantitation: a review, with an assessment of Tyramide signal amplification, multispectral imaging and multiplex analysis. Methods 2014;70(1):46–58. doi:10.1016/j.ymeth.2014.08.016, PMID:25242720.
[30] Tao Y, Wang Y, Wang M, Tang H, Chen E. Mesenchymal Stem Cells Alleviate Acute Liver Failure through Regulating Hepatocyte Apoptosis and Macrophage Polarization. J Clin Transl Hepatol 2024;12(6):571–580. doi:10.14218/JCTH.2023.00557, PMID:38974955.
[31] Love MI, Huber W, Anders S. Moderated estimation of fold change and dispersion for RNA-seq data with DESeq2. Genome Biol 2014;15(12):550. doi:10.1186/s13059-014-0550-8, PMID:25516281.
[32] Subramanian A, Tamayo P, Mootha VK, Mukherjee S, Ebert BL, Gillette MA, *et al*. Gene set enrichment analysis: a knowledge-based approach for interpreting genome-wide expression profiles. Proc Natl Acad Sci U S A 2005;102(43):15545–15550. doi:10.1073/pnas.0506580102, PMID:16199517.
[33] Liberzon A, Birger C, Thorvaldsdóttir H, Ghandi M, Mesirov JP, Tamayo P. The Molecular Signatures Database (MSigDB) hallmark gene set collection. Cell Syst 2015;1(6):417–425. doi:10.1016/j.cels.2015.12.004, PMID:26771021.
[34] Jia Y, Ma L, Wang Y, Wang W, Shen C, Wang X, *et al*. NLRP3 inflammasome and related cytokines reflect the immune status of patients with HBV-ACLF. Mol Immunol 2020;120:179–186. doi:10.1016/j.molimm.2020.01.011, PMID:32169738.
[35] Laleman W, Claria J, Van der Merwe S, Moreau R, Trebicka J. Systemic Inflammation and Acute-on-Chronic Liver Failure: Too Much, Not Enough. Can J Gastroenterol Hepatol 2018;2018:1027152. doi:10.1155/2018/1027152, PMID:30155448.
[36] Tan N, Jian G, Peng J, Tian X, Chen B. Chishao - Fuzi herbal pair restore the macrophage M1/M2 balance in acute-on-chronic liver failure. J Ethnopharmacol 2024;328:118010. doi:10.1016/j.jep.2024.118010, PMID:38499260.
[37] He L, Cai Q, Liang X, Xin J, Shi D, Ren K, *et al*. ETS2 alleviates acute-on-chronic liver failure by suppressing excessive inflammation. J Med Virol 2023;95(4):e28710. doi:10.1002/jmv.28710, PMID:36975761.
[38] He J, Li X, Zhou J, Hu R. BATF2 and PDK4 as diagnostic molecular markers of sarcoidosis and their relationship with immune infiltration. Ann Transl Med 2022;10(2):106. doi:10.21037/atm-22-180, PMID:35282063.
[39] Chen T, Ye L, Zhu J, Tan B, Yi Q, Sun Y, *et al*. Inhibition of Pyruvate Dehydrogenase Kinase 4 Attenuates Myocardial and Mitochondrial Injury in Sepsis-Induced Cardiomyopathy. J Infect Dis 2024;229(4):1178–1188. doi:10.1093/infdis/jiad365, PMID:37624974.
[40] Zheng X, Huang J, Meng J, Wang H, Chen L, Yao J. Identification and Experimental Verification of PDK4 as a Potential Biomarker for Diagnosis and Treatment in Rheumatoid Arthritis. Mol Biotechnol 2025;67(10):3975–3992. doi:10.1007/s12033-024-01297-1, PMID:39466354.
[41] Forteza MJ, Berg M, Edsfeldt A, Sun J, Baumgartner R, Kareinen I, *et al*. Pyruvate dehydrogenase kinase regulates vascular inflammation in atherosclerosis and increases cardiovascular risk. Cardiovasc Res 2023;119(7):1524–1536. doi:10.1093/cvr/cvad038, PMID:36866436.
[42] Min BK, Park S, Kang HJ, Kim DW, Ham HJ, Ha CM, *et al*. Pyruvate Dehydrogenase Kinase Is a Metabolic Checkpoint for Polarization of Macrophages to the M1 Phenotype. Front Immunol 2019;10:944. doi:10.3389/fimmu.2019.00944, PMID:31134063.
[43] Han X, Ma W, Zhu Y, Sun X, Liu N. Advanced glycation end products enhance macrophage polarization to the M1 phenotype via the HIF-1α/PDK4 pathway. Mol Cell Endocrinol 2020;514:110878. doi:10.1016/j.mce.2020.110878, PMID:32464167.
[44] Zhou J, Yang Z, Yang X, Wang Z. Changes in TNF-α, IL-33, and MIP-1α before and after artificial liver support treatment and their prognostic value. Am J Transl Res 2024;16(3):988–997. doi:10.62347/CBKR4894, PMID:38586093.
[45] Dimitriadis K, Katelani S, Pappa M, Fragkoulis GE, Androutsakos T. The Role of Interleukins in HBV Infection: A Narrative Review. J Pers Med 2023;13(12):1675. doi:10.3390/jpm13121675, PMID:38138902.
[46] Zhu B, Gao F, Li Y, Shi K, Hou Y, Chen J, *et al*. Serum cytokine and chemokine profiles and disease prognosis in hepatitis B virus-related acute-on-chronic liver failure. Front Immunol 2023;14:1133656. doi:10.3389/fimmu.2023.1133656, PMID:37180134.
[47] Wang J, Liu Y, Ding H, Shi X, Ren H. Mesenchymal stem cell-secreted prostaglandin E(2) ameliorates acute liver failure via attenuation of cell death and regulation of macrophage polarization. Stem Cell Res Ther 2021;12(1):15. doi:10.1186/s13287-020-02070-2, PMID:33413632.
[48] Sun P, Li Z, Yan Z, Wang Z, Zheng P, Wang M, *et al*. Lenvatinib targets STAT-1 to enhance the M1 polarization of TAMs during hepatocellular carcinoma progression. BMC Cancer 2024;24(1):922. doi:10.1186/s12885-024-12680-1, PMID:39080642.
[49] Vandsemb EN, Rye MB, Steiro IJ, Elsaadi S, Rø TB, Slørdahl TS, *et al*. PRL-3 induces a positive signaling circuit between glycolysis and activation of STAT1/2. FEBS J 2021;288(23):6700–6715. doi:10.1111/febs.16058, PMID:34092011.
[50] Yang CS, Kim JJ, Lee SJ, Hwang JH, Lee CH, Lee MS, *et al*. TLR3-triggered reactive oxygen species contribute to inflammatory responses by activating signal transducer and activator of transcription-1. J Immunol 2013;190(12):6368–6377. doi:10.4049/jimmunol.1202574, PMID:23670194.